Comparative analysis of tropospheric delay models using reference data derived from ray tracing numerical weather model

Szabolcs Rózsa[1], Bence Ambrus[2], Ildikó Juni[3]
Department of Geodesy and Surveying
Budapest University of Technology and Economics, Faculty of Civil Engineering
Budapest, Hungary
[1]rozsa.szabolcs@epito.bme.hu, [2]ambrus.bence@epito.bme.hu, [3]juni.ildiko@epito.bme.hu

***Abstract*—Electromagnetic signals broadcast by GNSS satellites suffer considerable delays while travelling through the atmosphere. The tropospheric delay depends on the actual meteorological parameters of the atmosphere and also on the elevation angles of the satellites. There are numerous models for calculating the tropospheric delay, however, these models deviate quite significantly from each other, either in the meteorological parameters used during the calculation or whether they take into account the periodic perturbation of some meteorological parameters. We studied the wet and hydrostatic part of the tropospheric delay separately and also differentiated between blind and site mode of all the models. In blind mode the model uses its own meteorological dataset while in site mode in situ measurements of the parameters are applied. Our goal was to test the accuracy of four troposphere models, employing the ray tracing method, using input data from numerical weather models. For the analysis we calculated statistical parameters to evaluate the performance of each model.**

Keywords—troposphere, tropospheric delay, GNSS, ESA, GPT2, GPT2w, RTCA-MOPS, ray tracing, numerical weather model

I. Introduction

Using the global navigation satellite systems is becoming part of more and more walks of our everyday life. The troposphere and the electrically neutral zone above it in the atmosphere cause significant signal delays in GNSS observations. The tropospheric delay can be separated into two parts, the hydrostatic and the wet delay. Both of these can be calculated using different delay models. Our aim in this paper is to analyse four tropospheric delay models: the RTCA-MOPS [1], the model developed by ESA for the Galileo satellite system [2], the GPT2 [3] and GPT2w [4] models developed by the Technical University of Vienna. In order to do this, we created a reference model, using input data from a numerical weather model for the period of 2010-2011 and a ray tracing algorithm. Besides the meteorological parameters, the tropospheric delay depends on the elevation angle of the observed satellite as well, so in the analysis we studied the model performance in different elevation angles: 3°, 5°, 10°, 45° and 90°.

II. The effect of the troposphere and the models used in the study

The tropospheric delay effect comes from the change in refractivity along the signals propagation path. The total tropospheric delay can be calculated with the Thayer-integral [5], using (1):

$$T = 10^{-6} \int N \, ds \tag{1}$$

where N denotes the refractivity. The total tropospheric delay in zenith direction (ZTD) can be divided into two parts, the hydrostatic delay in zenith direction (ZHD), which is the effect of gases in hydrostatic equilibrium and the wet delay in zenith direction (ZWD) which is caused by the water vapour content of the air. ZHD and ZWD depend on different meteorological parameters in different tropospheric models, such as pressure, temperature, water vapour pressure, temperature lapse rate, water vapour lapse rate and so on. We have to take into account the elevation angle of the satellite, because the delay grows significantly if the satellite is closer to the horizon. The delay is usually calculated in the zenith direction and then converted to any slant direction, using a mapping function. When calculating with different troposphere models, we have to distinguish between blind mode and site mode. The models use their own built-in meteorological data in blind mode and apply user supplied measurements of meteorological parameters in site mode to improve the model performance in ground based augmentation systems. In our analysis, both operation modes were used for each model.

A. RTCA-MOPS model

The tropospheric delay TD_i for satellite i takes the form described in [1], using the following formula:

$$TD_i = (ZHD + ZWD) \cdot m(E_i) \tag{2}$$

where $m(E_i)$ is the mapping function to scale the delays to the satellite's elevation angle.

ZHD and *ZWD* are calculated from the receiver's height above the mean sea level, refraction coefficients, the gas

constant of dry air, the mean gravitational acceleration, and five meteorological parameters: air pressure, air temperature, water vapour pressure, temperature lapse rate and water vapour lapse rate. In blind mode the values of each of the five meteorological parameters, applicable to the receiver latitude and day of year (starting with 1 January), are computed from the average and annual variation values which are built into the model. The model calculates and applies the mapping function described in [6] to give the total delay, which is valid for satellite elevation angles not less than 4°. If the elevation angle is less than 4° but not less than 2°, an expanded version of the formula is used.

B. ESA model

The calculation of the zenith hydrostatic and the zenith wet delays for a receiver on the surface is similar to the method used in the RTCA-MOPS model [2]. In contrast however, the gravity acceleration is not a constant anymore, but rather a function of latitude and height of the receiver above mean sea level. Tropospheric hydrostatic and wet delays are calculated in the zenith direction. In order to obtain the tropospheric delay for any elevation angle, the Niell mapping function [7] is applied. The input parameters for the ESA-model in blind mode are derived from a re-analysis dataset of the European Centre for Medium-Range Weather Forecasts (ECMWF), the ERA15 statistical analysis and stored in climatological maps. In total 21 maps are utilized, where the mean values, daily and annual fluctuations of all the climate parameters are given. The tropospheric delay at any receiver position is calculated using bilinear interpolation based on delay values at the four closest grid points surrounding the receiver.

C. GPT2 model

The GPT2 (Global Pressure and Temperature Model) is a global empirical model of surface meteorological parameters. GPT2 provides pressure, temperature, temperature lapse rate, water vapour pressure and mapping function coefficients [3]. The Vienna Mapping Function 1 (VMF1) [8] is used to transform the zenith delay into slant delay. In blind mode, when only the coordinates of the station and the date of the observation are given, all the meteorological parameters are calculated from the model. In this case, the mean values, annual and semi-annual variations of all the hydrostatic climate parameters are given on a global grid with a resolution of 1° x 1°. The meteorological data are derived from ECMWF Re-Analysis monthly mean profiles between 2001-2010 using 37 pressure levels. These meteorological parameters are then used as input data for the Saastamoinen troposphere model [9] to calculate the hydrostatic part of the delay and the Askne-Nordius troposphere model [10] in order to calculate the wet part of the delay.

D. GPT2w

The GPT2w [4] is an upgraded version of the GPT2, providing mean values, annual and semi-annual variations for pressure, temperature, temperature lapse rate, water vapour pressure and its decrease factor, weighted mean temperature as well as hydrostatic and wet mapping function coefficients for the VMF1. The model uses a global grid of a resolution of 1° x 1° to store the mean values, annual and semi-annual variations of the hydrostatic and wet climatological parameters used in blind mode. The hydrostatic delay can be calculated like in the case of GPT2 and the wet tropospheric delay is determined using the Askne-Nordius formula [10].

III. Generating the reference data using ray tracing

A. Input data

ECMWF ERA-Interim monthly mean solutions were used for both the ray tracing and in the site mode computation for the different troposphere models. The dataset contained relative humidity, temperatures and geopotential values for 37 pressure levels, ranging from 1000 hPa to 1 hPa. The mean values for each month are computed and interpolated onto a global grid with a resolution of 1° x 1°. The ERA-Interim data is expanded up to the height of 86 km with values given in the International Standard Atmosphere (ISA).

B. The ray tracing algorithm

Using this method, the path of a satellite beam is traced throughout the neutral atmosphere, starting at a certain elevation angle and continuously refracting at different layers of the atmosphere Besides calculating the total length of the path the refracted beam takes (which gives us the geometric delay), we also compute the hydrostatic and wet refractivity values of each layer and use them in (3).

In order to achieve accurate results with ray tracing, the resolution of the input data must be increased [8]. The resolution of the height used for the interpolation varies according to the gradient of the interpolant parameter in a pre-defined manner. The interpolation is done linearly for the temperature and exponentially for the air pressure and water vapour pressure values. If the lowest pressure level is located above the topography, an extrapolation step is carried out using the values of the two pressure levels that are closest to the surface in order to start every ray tracing computation from the level of the topography.

In the next step the hydrostatic and wet refractivity values are calculated. The total refractivity at each level is the sum of the hydrostatic and wet parts [11]. From these values, we can derive the length of the refracted beam in each layer. The distance travelled by the ray and therefore the delay caused by the troposphere can be calculated using the refractivity of each layer and the distance travelled by the beam in that given layer:

$$ds_h = \sum_{i=1}^{k-1} s_i \cdot N_{h,i} \qquad ds_w = \sum_{i=1}^{k-1} s_i \cdot N_{\mathrm{w},i} \tag{3}$$

In the formula s_i is the length of the refracted beam, $N_{h,i}$ is the hydrostatic refractivity and $N_{w,i}$ is the wet refractivity in the i-th layer.

As a result of the ray tracing computation, a global grid was created with a resolution of 1° x 1° for each month (24 in total), using the vertical profiles obtained from the numerical weather data. For each grid point, the hydrostatic and wet tropospheric delay values were determined. These grids served as the reference of the comparison for each troposphere model.

IV. Comparative Analysis of the Troposphere Models

A. Statistical parameters used in the analysis

Having created the reference dataset, we had a common basis to which each of the troposphere models could be compared. In order to assess the goodness of the models, three different statistical characteristics were calculated from the data. The input generated to be used in the computations was the differences ($d_i = D_{r,i} - D_{m,i}$) between the reference delay values ($D_{r,i}$) obtained with ray tracing and the delay values calculated using the various troposphere models ($D_{m,i}$). The bias of the model denoted the arithmetic mean of the differences. In addition to this, we computed the root mean square and the corrected standard deviation for each model.

The statistical parameters were calculated for both blind and site operation modes of each of the models using a two year dataset (2010-2011) with one sample per month. The delay values were calculated for the elevation angles of 3°, 5°, 10°, 45° and 90°. The bias and the σ values were computed for every grid point of a worldwide grid with a resolution of 1° x 1°, while the RMS was represented for each model and operation mode by a single average value. When operated in site mode, we calculated the weather parameters on the ground level using the method described in section III/B.

In the following section of the paper, we present the results of the comparisons for each of the troposphere models and their operation modes.

B. Comparison of the troposphere models to the ray tracing data

1) RTCA-MOPS model

As the model only contains the annual variation of the meteorological parameters, the expected results of comparing the RTCA-MOPS model to the ray tracing dataset were moderate at best. The blind mode results show heavy biases for the wet delays in an approx. 30° wide swath around the equator (Fig. 1), which only start to disappear above 10° of elevation.

The σ and RMS values become substantial at lower elevation angles for both the hydrostatic and the wet delays and tend towards zero around 45° elevation (Table I.), however, the σ of the wet part of the delay remains relatively high around the equator.

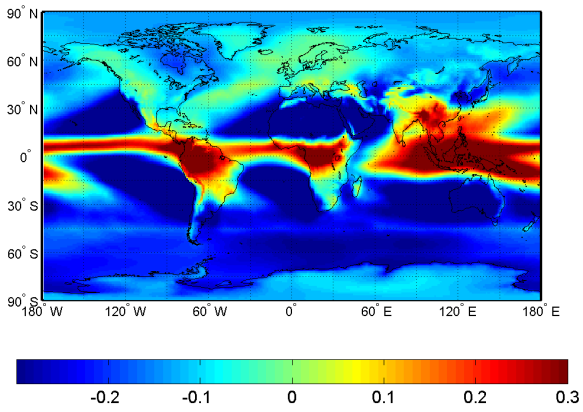

Fig. 1. Bias values of the wet delay from the RTCA-MOPS model at the elevation angle of 10°, computed using blind mode.

In good agreement with the expectations, the site mode results show considerable improvements of both the bias (Fig. 1), σ and the RMS values of the hydrostatic delay (Table I.). While there is noticeable development regarding the statistical parameters of the wet delay, both values remain rather significant along the equator.

Table I. below shows the RMS values of the hydrostatic and wet delays calculated from the RTCA-MOPS model for both operation modes.

TABLE I. RMS values of the RTCA-MOPS model in meters

Operation mode and type of delay	Elevation angles				
	3°	*5°*	*10°*	*45°*	*90°*
Blind mode hydrostatic	1.210	0.568	0.221	0.041	0.028
Blind mode: wet	0.792	0.527	0.286	0.072	0.051
Site mode: hydrostatic	1.054	0.434	0.126	0.008	0.005
Site mode: wet	0.570	0.330	0.166	0.041	0.029

2) ESA model

The troposphere model developed by ESA improves upon the results of the RTCA-MOPS model. Its meteorological dataset contains not only the annual but the diurnal variations of the core parameters as well. In blind mode, the bias of the hydrostatic delays, while still high at lower elevation angles, diminishes around 10° (Fig. 2a). The decrease of the blind σ and RMS values becomes faster as well (Table II.). The bias of the wet delays calculated in blind mode is substantially lower than the values of the RTCA-MOPS model (Fig. 2b and Fig. 1), even at the elevation angle of 10°. The same trend can be noticed for the standard deviation as well.

Using the site mode of the model, further improvements can be noted in the hydrostatic delays. The bias becomes increasingly lower even at the elevation angle of 10° and while there is some fluctuation in the σ values at lower elevations, the results become consolidated at approx. 10° of elevation. As for the wet part of the tropospheric delay, both the bias and the σ values remain relatively high up to the elevation angle of 10° and decreasing to approx. the same levels as in blind mode at higher elevations (Table II.).

Table II. shows the calculated RMS values for each of the operation modes of the ESA model.

TABLE II. RMS values of the ESA model in meters

Operation mode and type of delay	Elevation angles				
	3°	*5°*	*10°*	*45°*	*90°*
Blind mode hydrostatic	0.697	0.266	0.085	0.017	0.012
Blind mode: wet	0.405	0.261	0.136	0.034	0.024
Site mode: hydrostatic	0.692	0.252	0.066	0.010	0.007
Site mode: wet	0.361	0.235	0.123	0.031	0.022

3) The GPT2 model

As described in Section II, when we talk about the GPT2 model, we mean the Saastamoinen [9] and the Askne-Nordius [10] troposphere models to calculate the hydrostatic and the wet parts of the delay respectively, using the meteorological parameters supplied by the GPT2 as input data. While the GPT2

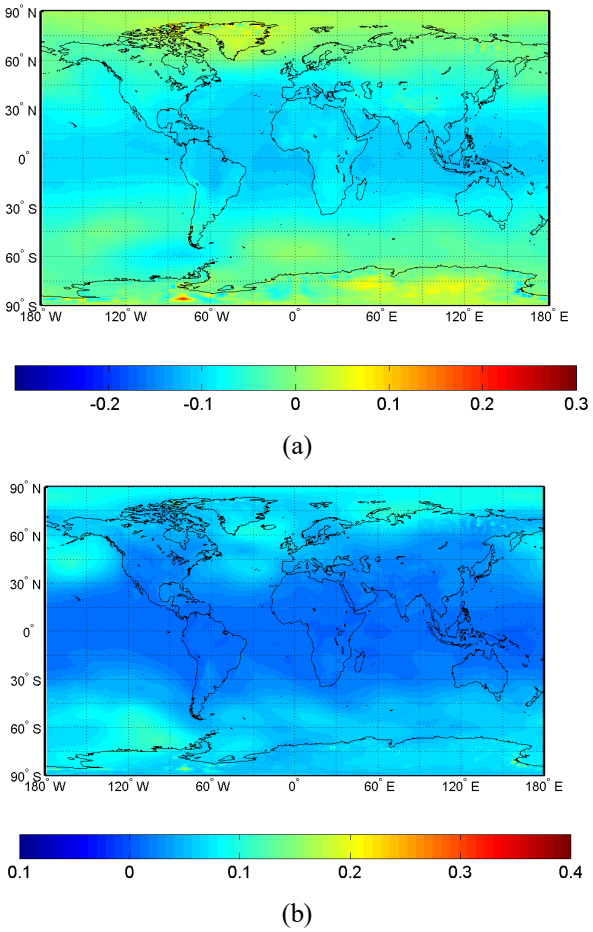

Fig. 2. Bias of the hydrostatic (a) and wet (b) parts of the tropospheric delay, calculated using the blind mode of the ESA model.

itself was developed after the ESA model, it cannot be considered a direct improvement on it. This is due to the fact, that even though it contains the annual and semi-annual variations of the parameters, this is only valid for the parameters used for the hydrostatic delay calculation.

The bias for the hydrostatic part computed in blind mode show little difference between the ESA model and GPT2, with the GPT2 being slightly more coherent at lower elevation angles. The σ values are practically identical for both troposphere models. As for the wet part calculated in blind mode, the bias of the GPT2 results are significantly higher up to 10° of elevation and remain so around the equator even above that. In terms of the σ values, little to no improvement can be noticed (Table III.).

Similar results can be seen when the model is used in site mode. The hydrostatic bias values show no development, while there is some improvement in coherence of the σ results. The higher bias values of the wet delays are more concentrated around the equator in case of the GPT2, as opposed to the ESA model and continue to remain higher at elevation angles above 10° as well. Similarly, the high σ values are condensed more noticeably in a 60° swath around the equator and remain slightly larger at higher elevation angles (Fig. 3).

According to the RMS values in Table III., even at higher elevation angles, the GPT2 model deviates slightly more from the reference data than the ESA model.

TABLE III. RMS VALUES OF THE GPT2 MODEL IN METERS

Operation mode and type of delay	Elevation angles				
	3°	*5°*	*10°*	*45°*	*90°*
Blind mode hydrostatic	0.724	0.275	0.085	0.017	0.012
Blind mode: wet	0.498	0.316	0.163	0.040	0.029
Site mode: hydrostatic	0.710	0.258	0.067	0.010	0.007
Site mode: wet	0.435	0.276	0.142	0.035	0.025

4) The GPT2w model

The GPT2w can be considered a direct improvement of the GPT2 model, with the aim of enhancing the accuracy of modelling the wet part of the tropospheric delay. The model contains the annual and semi-annual variations for the parameters used to calculate the wet part of the delay as well.

Comparing the bias of the hydrostatic delay calculated using the blind mode of the model to the ESA model, we receive similar results with the GPT2w having more consistent deviations from the reference dataset at lower elevation angles. The σ values show little difference as well. The improved wet delay modelling of the GPT2w shows significant improvement in the bias of the differences at lower elevation angles, however,

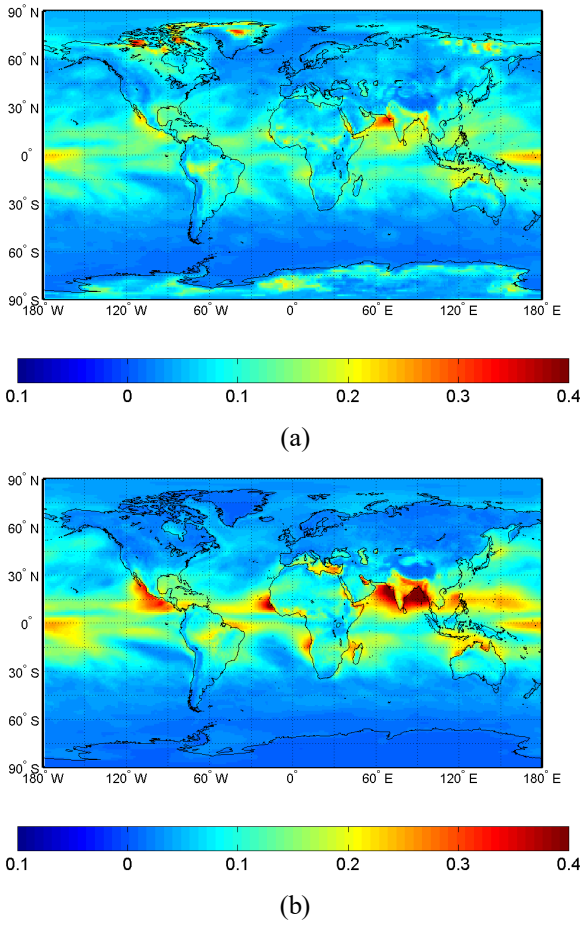

Fig. 3. σ values of the wet tropospheric delay computed using the ESA (a) and the GPT2 (b) models in site mode at the elevation angle of 10°.

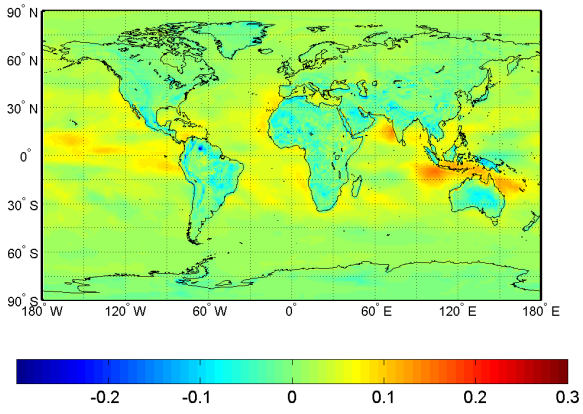

(a)

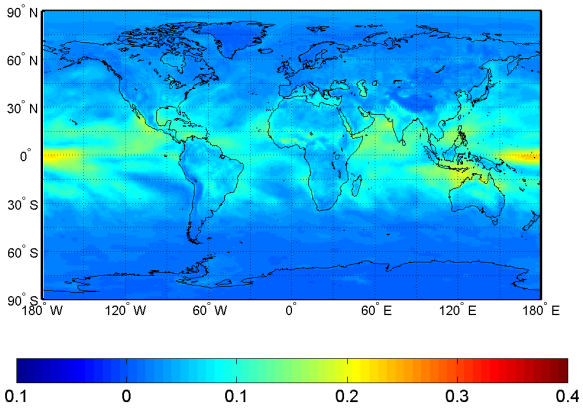

(b)

Fig. 4. Bias (a) and σ (b) values of the wet tropospheric delay computed using the site mode of the GPT2w model at the elevation angle of 10°.

it tends to remain a bit higher at the equatorial region than the ESA model. The σ values show the same trend, at lower elevation angles, the GPT2w indicates improvement compared to the ESA model, even though the results become rather similar at higher elevation angles.

When using the site mode of the model to calculate the hydrostatic delay, it shows little to no improvement compared to the ESA model or the GPT2 in terms of both bias and σ values. However, when modelling the wet part of the delay, the difference is quite significant with the GPT2w giving smaller bias values even at lower elevation angles. The σ values display improvement as well up to the elevation angle of 45°, above which the difference is no longer noticeable (Fig. 4).

The RMS values presented in Table IV. indicate that the model data from the GPT2w generally better resembles the reference dataset, however much of the improvement can be noted in modelling the wet part of the tropospheric delay in both blind and site modes.

TABLE IV. RMS VALUES OF THE GPT2W MODEL IN METERS

Operation mode and type of delay	Elevation angles				
	3°	*5°*	*10°*	*45°*	*90°*
Blind mode hydrostatic	0.719	0.272	0.083	0.016	0.012
Blind mode: wet	0.267	0.172	0.089	0.022	0.016
Site mode: hydrostatic	0.710	0.258	0.067	0.010	0.007
Site mode: wet	0.197	0.128	0.067	0.017	0.012

V. SUMMARY AND CONCLUSIONS

In the paper we presented the comparative analysis of troposphere delay models currently applied in high precision processing of GNSS observations. The reference dataset used in the study was generated employing a ray tracing algorithm and meteorological data from a numerical weather model as input. Comparing the computed delay from each model to the ray tracing data, we determined statistical parameters for every studied model to assess their quality. While the models produce increasingly good results at higher elevation angles, in case of integrity considerations, accurate performance at lower elevations is key. Out of the four models analysed in the paper, the troposphere model developed by ESA and the GPT2w model developed by the Technical University of Vienna proved to give results that best fit the reference dataset. Both models have similar characteristics concerning the hydrostatic part of the delay with the GPT2w supplying significantly improved results for the wet part of the tropospheric delay even at lower elevation angles.

REFERENCES

[1] "MOPS-DO-229D with Change 1 - Minimum Operational Performance Standards for Global Positioning System/Satellite-Based Augmentation System Airborne Equipment," Radio Technical Commission for Aeronautics, December 2006.

[2] A. Martelucci, ESA Galileo Programme, "Galileo Reference Troposphere Model for the user receiver," 2002, ESA-APPNG-REF/00621-AM, ver. 2.7, 2012

[3] K. Lagler, M. Schindelegger, J. Böhm, H. Krásná and T. Nilsson, "GPT2: Empirical slant delay model for radio space geodetic techniques," 2013, Geophysical Research Letters, 40(6), 1069-1073. doi: 10.1002/grl.50288

[4] J. Böhm, G. Möller, M. Schindelegger, G. Pain, and R. Weber, "Development of an improved empirical model for slant delays in the troposphere (GPT2w)," 2015, GPS Solutions, 19(3), 433-441. doi: 10.1007/s10291-014-0403-7

[5] J. Ádám, L. Bányai, T. Borza, Gy. Busics, A. Kenyeres, A. Krauter, B. Takács, "Műholdas helymeghatározás," Műegyetemi Kiadó, Budapest, 2004, pp. 100-103.

[6] H. D. Black and A. Eisner, "Correcting satellite Doppler data for tropospheric effects," 1984, Journal of Geophysical Research. 89, pp. 2616-2626

[7] A.E. Niell, "Global mapping functions for the atmosphere delay at radio wavelengths," 1996, J. Geophys. Res. 101(B2):3227-3246.

[8] J. Boehm and H. Schuh, " Vienna Mapping Functions," 2003, 16. Working Meeting on European VLBI for Geodesy and Astrometry 131-143.

[9] J. Saastamoinen,. "Atmospheric correction for the troposphere and stratosphere in radio ranging of satellites," 1972, The Use of Artificial Satellites for Geodesy, 15, pp. 247-251.

[10] J. Askne and H. Nordius, "Estimation of tropospheric delay for microwaves from surface weather data," 1987, Radio Science, 22, 379-386, DOI: 10.1029/RS022i003p00379

[11] E. K. Smith and S. Weintraub, "The constants in the equation for atmospheric refractive index at radio frequencies," 1953, Proceedings of the Institute of Radio Engineers 41, pp.1035-1037.